

Stochastic switching in slow-fast systems: a large fluctuation approach

Christoffer R. Heckman* and Ira B. Schwartz†

U.S. Naval Research Laboratory, Code 6792

Plasma Physics Division,

Nonlinear Dynamical Systems Section

Washington, DC 20375, USA

In this paper we develop a perturbation method to predict the rate of occurrence of rare events for singularly perturbed stochastic systems using a probability density function approach. In contrast to a stochastic normal form approach, we model rare event occurrences due to large fluctuations probabilistically and employ a WKB ansatz to approximate their rate of occurrence. This results in the generation of a two-point boundary value problem that models the interaction of the state variables and the most likely noise force required to induce a rare event. The resulting equations of motion of describing the phenomenon are shown to be singularly perturbed. Vastly different time scales among the variables are leveraged to reduce the dimension and predict the dynamics on the slow manifold in a deterministic setting. The resulting constrained equations of motion may be used to directly compute an exponent that determines the probability of rare events.

To verify the theory, a stochastic damped Duffing oscillator with three equilibrium points (two sinks separated by a saddle) is analyzed. The predicted switching time between states is computed using the optimal path that resides in an expanded phase space. We show that the exponential scaling of the switching rate as a function of system parameters agrees well with numerical simulations. Moreover, the dynamics of the original system and the reduced system via center manifolds are shown to agree in an exponentially scaling sense.

Keywords: singular perturbation, stochastic differential equation, optimal path, noise, rare event

I. INTRODUCTION

Many stochastic systems of physical interest possess dynamics which occur over multiple time scales. These systems present unique difficulties since the multiple time scales interact with the stochasticity to affect the dynamics, leading to phenomena such as stochastic switching resulting from large fluctuations. For deterministic slow-fast systems singular perturbation theory may be applied to guide analysis, while noisy systems are better understood through tools from statistical mechanics.

The study of slow-fast systems has recently become popular as a result of the insight it affords into fields such as chemical reactions and electro-mechanical systems [1]. Due to the presence of distinct timescales on which phenomena occur in these singularly perturbed systems, it becomes mathematically tractable to apply perturbation methods to accurately predict the behavior of high-order systems in terms of low order ones. This model reduction greatly simplifies bifurcation analysis and the identification of qualitative behaviors. The approach of perturbation methods is especially useful because the alternative, running large-scale numerical simulations from which one may calculate statistics, is particularly burdensome for slow-fast systems. Such systems generally require the use of implicit numerical integrators in order to ensure numerical stability, the use of which is extremely computationally expensive.

Separately, stochastic systems are frequently used to model both microscale and macroscale behaviors that are inherently noisy or simpler to visualize as driven by randomness. Examples of these systems range from networks of sensors in noisy environments to the control of epidemics. There are many intricacies under investigation within this field such as finite noise effects and stochastic resonance [2] that provide for much lively research, but will not be our focus in this paper. We will in particular study the effect of small noise on the escape times for a particle in a multi-scale potential well. To do so, we will make use of the variational theory of large fluctuations as it applies to finding the *most probable path* along which noise directs a particle to escape [3].

It is well-known that noise has a significant effect on deterministic dynamical systems. For example, consider a given initial state in the basin of attraction for a given attractor, which might be steady, periodic, or chaotic. Noise can cause the trajectory to cross the deterministic basin boundary and move into another, distinct basin of attraction [4–7]. For sufficiently small noise, basin boundary crossings usually occur near a saddle on the boundary. However we note that for large noise, such a crossing may be determined by the global manifold structure away from the saddle.

This paper will consider small noise effects in particular. Specifically, we will investigate the effect of arbitrarily small noise on the escape of a particle from a potential well. In the small noise limit, one can apply large fluctuation theory [4, 5, 7, 8]; also known as large deviation theory used in white noise analysis [8–10], this approach enables us to determine the first passage times in a multi-scale environment. For a vector field that ex-

* christoffer.heckman.ctr@nrl.navy.mil

† ira.schwartz@nrl.navy.mil

hibits dynamics on only one timescale, it is clear how to use the theory to generate an optimal path of escape. The theory has been applied to a variety of Hamiltonian and Lagrangian variational problems [9, 11–16] that do not exhibit singularly perturbed behavior.

For slow-fast systems however, technical issues arise while determining the projection of noise restricted to the lower dimensional manifold. Several sample based approaches have been developed to understand dimension reduction in systems that have well separated time scales [17]. The existence of a stochastic center manifold was proven in [18] for systems with certain spectral requirements. Non-rigorous stochastic normal form analyses (which lead to the stochastic center manifold) were performed in [19–21]. More rigorous theoretical treatments of normal form coordinate transformations for stochastic center manifold reduction were developed in [22–24]. Later, another method of stochastic normal form reduction was developed in which anticipatory convolutions (integrals into the future of the noise processes) that appeared in the equations for the slow dynamics were ignored [25]. This latter stochastic normal form technique was possible because the epidemic model under study permitted certain assumptions on the magnitude of the noise projections. The disadvantage of such assumptions compared to probabilistic methods is that there must be guarantees to keep stochastic solutions bounded in the past and future [26], which we may not always have.

We will restrict our study to systems with two stable equilibria separated by an unstable equilibrium point in phase space; the method of center manifold approximations however is not strictly reserved for this case. This paper begins by introducing some general theory related to slow-fast systems and center manifold reductions. We then review large fluctuation theory and how it applies to determining the optimal path between invariant manifolds in stochastic systems. Next we follow many other works and apply the theory to the example of a damped Duffing oscillator to compare. Finally we compare the switching time estimated via large fluctuation theory with numerical results for the example system. We note that although much work on white noise model reduction is being done using sample-based methods and asymptotics, our variational approach is more general in that it may include non-Gaussian noise sources as well.

II. THEORY

We consider a general $(m+n)$ -dimensional dynamical system of stochastic differential equations with two well-separated timescales and additive noise on the slow variables:

$$\dot{\mathbf{x}} = \mathbf{F}(\mathbf{x}, \mathbf{y}) + \Phi(t) \quad (1)$$

$$\epsilon \dot{\mathbf{y}} = \mathbf{G}(\mathbf{x}, \mathbf{y}) \quad (2)$$

where $\mathbf{x} \in \mathbb{R}^m$, $\mathbf{y} \in \mathbb{R}^n$; $\Phi(t)$ are stochastic terms with characteristics depending on the application; $\mathbf{F} : \mathbb{R}^m \times \mathbb{R}^n \rightarrow \mathbb{R}^m$ and $\mathbf{G} : \mathbb{R}^m \times \mathbb{R}^n \rightarrow \mathbb{R}^n$ are differentiable functions with equilibrium points at the origin, and ϵ is a small parameter. Such systems are known as singularly perturbed or slow-fast systems [27] with timescales separated by a ratio of ϵ . In this system, \mathbf{x} are slow variables and \mathbf{y} are fast variables. Rescaling $\tau = \epsilon t$ and temporarily removing the stochastic terms results in the *layer equations*. Denoting $(\cdot)' = \frac{d}{d\tau}$, the deterministic part of Eqs. (1), (2) becomes:

$$\mathbf{x}' = \epsilon \mathbf{F}(\mathbf{x}, \mathbf{y}) \quad (3)$$

$$\mathbf{y}' = \mathbf{G}(\mathbf{x}, \mathbf{y}) \quad (4)$$

$$\epsilon' = 0. \quad (5)$$

Note that since ϵ is treated as a state variable in Eqs. (3)–(5), then all terms in Eq. (3) are necessarily nonlinear. If $\mathbf{G}(\mathbf{x}, \mathbf{y})$ has a linear part with nonzero determinant, then there exists an m -dimensional center manifold tangent to the center eigenspace at the origin. By the implicit function theorem, we may write the manifold locally as a function $\mathbf{h} : \mathbb{R}^m \times \mathbb{R} \rightarrow \mathbb{R}^n$:

$$\mathbf{y} = \mathbf{h}(\mathbf{x}, \epsilon). \quad (6)$$

Following Carr [28], the center manifold may be approximated to arbitrary order by a polynomial series in \mathbf{x} and ϵ . All solutions collapse to this manifold at an exponential rate since it is hyperbolic.

A. Stochastic switching

Stochastic differential equations cannot be described by deterministic orbits representing trajectories of a particle through phase space. Instead, other approaches are used to qualitatively describe the system. For instance, sample based techniques may describe individual realizations in phase space, or families of such realizations. Another technique is to find a probability density function (pdf) describing the likelihood of finding a particle at a given point and time. If the noise is Gaussian and uncorrelated in time, the dynamics of the pdf $\rho(\mathbf{z}, t)$, where $\mathbf{z} = (\mathbf{x}; \mathbf{y})$ is the concatenated vector of state variables, are governed by the Fokker-Planck equation [29]:

$$\begin{aligned} \frac{\partial \rho(\mathbf{z}, t)}{\partial t} = & - \sum_{i=1}^{m+n} \frac{\partial}{\partial z_i} (\rho(\mathbf{z}, t) \mathcal{F}_i) \\ & + \sum_{i=1}^{m+n} \sum_{j=1}^{m+n} \frac{\partial^2}{\partial z_i \partial z_j} (D_{ij} \rho(\mathbf{z}, t)) \end{aligned} \quad (7)$$

where $\mathcal{F} = (\mathbf{F}; \mathbf{G})$ is the concatenated vector of functions describing the vector field and D_{ij} is a diffusion coefficient matrix.

Equation (7) relates the time derivative of the probability density function $\rho(\mathbf{z}, t)$ with expressions involving spatial derivatives of the vector field \mathcal{F} . Presuming the characterization of the noise and the vector fields are autonomous, the pdf will asymptotically approach a steady state distribution that is independent of time. Therefore, we seek steady state solutions to Eq. (7); that is,

$$\sum_{i=1}^{m+n} \frac{\partial}{\partial z_i} (\rho(\mathbf{z}) \mathcal{F}_i) = \sum_{i=1}^{m+n} \sum_{j=1}^{m+n} \frac{\partial^2}{\partial z_i \partial z_j} (D_{ij} \rho(\mathbf{z})). \quad (8)$$

If the intensity for each noise term is equal and each component is uncorrelated, then we may write $D_{ij} = D\delta_{ij}$. For the system described in Eqs. (1), (2), it is also relevant that $D_{ij}|_{i,j>m} = 0$ since additive noise only affects the slow variables; this results in

$$\sum_{i=1}^{m+n} \frac{\partial}{\partial z_i} (\rho(\mathbf{z}) \mathcal{F}_i) = D \sum_{i=1}^m \frac{\partial^2}{\partial z_i^2} \rho(\mathbf{z}). \quad (9)$$

We will now assume a certain form for the pdf that will allow us to solve Eq. (9) keeping in mind that the goal is to analyze stochastically-induced switching. In the small-noise limit, transitions between attractors happen only rarely. Therefore, noise leading to a transition is considered to be in the tail of the probability distribution that governs the amplitude of the noise. A stochastically-induced switch is *most likely* to occur in the presence of a hypothesized “optimal noise,” which has a finite likelihood of occurrence. The path that the system travels through phase space under the influence of the optimal noise is known as the “optimal path.” Such an event follows an exponential distribution which we will use as an ansatz to solve Eq. (9). The WKB ansatz states that $\rho(\mathbf{z}) \propto \exp(-\frac{1}{2D}R(\mathbf{z}))$. Applying this to the steady-state Fokker-Planck equation (9) yields the differential equation

$$\sum_{i=1}^{m+n} -\frac{\partial R}{\partial z_i} \mathcal{F}_i + 2D \frac{\partial \mathcal{F}_i}{\partial z_i} = \sum_{i=1}^m -D \frac{\partial R}{\partial z_i^2} + \frac{1}{2} \left(\frac{\partial R}{\partial z_i} \right)^2.$$

Since we are operating in the small-noise limit, any terms multiplied by D will be small; for now, we will neglect them leaving the first order nonlinear equation:

$$\sum_{i=1}^{m+n} -\frac{\partial R}{\partial z_i} \mathcal{F}_i = \frac{1}{2} \sum_{i=1}^m \left(\frac{\partial R}{\partial z_i} \right)^2. \quad (10)$$

In some cases, solving for R in Eq. (10) is possible and would result in a stationary pdf for Eqs. (1), (2). However, combined with the results in the following section, we will demonstrate that not only is there a straightforward way to tackle solving for R but also that it is intimately related with the principle of least action and the formulation of an optimal path.

B. Formulation of the Optimal Path

We wish to study the transition rates due to stochastic fluctuation between two energy minima. Consider a system with two stable equilibrium points \mathbf{z}_1 and \mathbf{z}_2 with a saddle point \mathbf{z}_s separating them. Since the noise intensity D is small, we assume that switching between the two states will be considered a “rare event.” The frequency of such an event is approximately determined by the most likely noise to bring the system from \mathbf{z}_1 to \mathbf{z}_s , i.e. the optimal noise. A realization of the optimal noise is calculated to guide the particle to the saddle point \mathbf{z}_s , which corresponds to the mean first passage time (MFPT). The method to calculate this path makes use of Hamiltonian’s principle. One may predict the switching rate by first finding the optimal path between the two states in an expanded phase space which accounts for the noise and then calculating the dynamical quantity known as the action along that path. For a rigorous explanation of this procedure, see [13, 30].

The optimal path is the path that is of minimal action. We write the action of the noise on the system (1), (2) as:

$$\begin{aligned} \mathcal{R}[\mathbf{x}, \mathbf{y}, \Phi, \lambda_x, \lambda_y] = & \frac{1}{2} \int \Phi(t) \cdot \Phi(t) dt \\ & + \int \lambda_x \cdot (\dot{\mathbf{x}} - \mathbf{F}(\mathbf{x}, \mathbf{y}) - \Phi(t)) dt \\ & + \int \lambda_y \cdot (\epsilon \dot{\mathbf{y}} - \mathbf{G}(\mathbf{x}, \mathbf{y})) dt. \end{aligned} \quad (11)$$

The action integral Eq. (11) represents the total effect of noise on the system subject to the constraints of the vector field. The first term involving the action of the noise is derived by taking a WKB approximation of the Chapman-Kolmogorov equation [3] for the infinitesimal noise events along the path for white noise. The λ factors are Lagrange multipliers, and the terms multiplying them are the constraint equations. The integral is calculated along the path for all time. We note that Eq. (11) is a natural way to describe the effects of noise from both white and non-Gaussian sources.

To find the functions that minimize the action, we take the first variation of the above equation with respect to the independent variables and set them equal to zero. This will give five sets of equations that when solved will extremize the action \mathcal{R} . An example of these variational calculations (with variation $\xi \in C^1$ bounded) on the action with respect to the functions x_i is:

$$\begin{aligned} \frac{\delta \mathcal{R}}{\delta x_i} = & \int \lambda_{x_j} \left(\dot{\xi} - \xi \frac{\partial F_j}{\partial x_i} \right) dt + \int \lambda_{y_j} \left(-\xi \frac{\partial G_j}{\partial x_i} \right) dt \\ = & \int \xi \left(-\dot{\lambda}_{x_i} - \lambda_{x_j} \frac{\partial F_j}{\partial x_i} - \lambda_{y_j} \frac{\partial G_j}{\partial x_i} \right) dt = 0. \end{aligned} \quad (12)$$

Arriving at the second equality involves integrating by parts; since the functional derivative restricts the varia-

tions ξ to be bounded, the first term arising from integration by parts vanishes. Given Eq. (12), we have that the function multiplying ξ in the integrand must vanish; this yields the differential equation:

$$\dot{\lambda}_{x_i} + \lambda_{x_j} \frac{\partial F_j}{\partial x_i} + \lambda_{y_j} \frac{\partial G_j}{\partial x_i} = 0. \quad (13)$$

In the same way, the following equations were derived for the first variation with respect to y_i , λ_{x_i} , λ_{y_i} and Φ_i :

$$\frac{\delta \mathcal{R}}{\delta y_i} = 0 \implies \epsilon \dot{\lambda}_{y_i} + \lambda_{y_j} \frac{\partial G_j}{\partial y_i} + \lambda_{x_j} \frac{\partial F_j}{\partial y_i} = 0 \quad (14)$$

$$\frac{\delta \mathcal{R}}{\delta \lambda_{y_i}} = 0 \implies \epsilon \dot{y}_i = G_i \quad (15)$$

$$\frac{\delta \mathcal{R}}{\delta \lambda_{x_i}} = 0 \implies \dot{x}_i = F_i + \Phi_i \quad (16)$$

$$\frac{\delta \mathcal{R}}{\delta \Phi_i} = 0 \implies \Phi_i = \lambda_{x_i} \quad (17)$$

where $i = 1, \dots, m$ and $i = 1, \dots, n$ for the slow and fast variables and their conjugate momenta respectively.

To make a connection with Section II A, we will for a moment consider the singular limit as $\epsilon \rightarrow 0$ of the vector field in Eqs. (14)–(17). This approximation describes the behavior of a particle in the x_i and λ_{x_i} coordinates after fast transients have died out and yields a system known as the “slow equations.” The slow equations are:

$$\dot{x}_i = F_i + \lambda_{x_i} \quad (18)$$

$$\dot{\lambda}_{x_i} = -\frac{\partial F_j}{\partial x_i} \lambda_{x_j}. \quad (19)$$

The slow equations represent a conservative system. To calculate the corresponding Hamiltonian, we note that:

$$\dot{x}_i = \frac{\partial \mathcal{H}}{\partial \lambda_{x_i}}$$

$$\dot{\lambda}_{x_i} = -\frac{\partial \mathcal{H}}{\partial x_i}$$

where the Hamiltonian is:

$$\mathcal{H} = F_i \lambda_{x_i} + \frac{1}{2} \lambda_{x_i} \lambda_{x_i}. \quad (20)$$

Setting $\mathcal{H} = 0$ in Eq. (20) verifies an intriguing relationship: if one identifies $\lambda_{x_i}(\mathbf{x}) = \frac{\partial R(\mathbf{x})}{\partial x_i}$, Eq. (20) and Eq. (10) are equivalent for the singular case. This confirms our earlier analysis using variational calculus and verifies that $R(\mathbf{z})$ in the Eikonal approximation is indeed the action.

The probability of a rare event occurring described by that approximation is directly proportional to the

switching rate, or its inverse, the mean first passage time. This quantity, denoted T_S is inversely proportional to the switching rate. Since the action will be calculated along the optimal path, $R = \min \mathcal{R}$ and the relation to the switching time is

$$T_S = c \exp(R/2D). \quad (21)$$

Since the switching rate is proportional to the probability of a large fluctuation, there is a proportionality constant c that is yet to be determined. The calculation of this prefactor is the subject of ongoing research [31], but is not the focus of the current work.

III. APPLICATION: THE DAMPED DUFFING OSCILLATOR

To test the method, we consider a prototypical example for a double-welled potential—the damped Duffing oscillator. A stochastic variant of this oscillator is:

$$\dot{x} = y + \eta(t) \quad (22)$$

$$\epsilon \dot{y} = x - x^3 - y \quad (23)$$

where ϵ is a small parameter and $\eta(t)$ is a noise source. We will consider the case where $\eta(t)$ represents uncorrelated Gaussian white noise and is defined by

$$\langle \eta(t)\eta(t') \rangle = 2D\delta(t-t').$$

The noise intensity, which controls the width of the distribution of noise, is represented by $D = \sigma^2/2$ where σ is the standard deviation of the noise.

Applying Eqs. (14)–(17) to this system, the variational equations for the damped Duffing oscillator in Eqs. (22)–(23) are:

$$\dot{\lambda}_1 = (3x^2 - 1)\lambda_2 \quad (24)$$

$$\epsilon \dot{\lambda}_2 = \lambda_2 - \lambda_1 \quad (25)$$

$$\epsilon \dot{y} = x - x^3 - y \quad (26)$$

$$\dot{x} = y + \lambda_1 \quad (27)$$

Following the language of Kaper [32], there are two limits over which the system in Eqs. (24)–(27) may be studied. The first involves immediately taking the limit as $\epsilon \rightarrow 0$ in the equations, while the latter involves a rescaling of time and will be considered in the following section. The first limit yields the slow equations; they are:

$$\dot{\lambda}_1 = (3x^2 - 1)\lambda_1 \quad (28)$$

$$\dot{x} = x - x^3 + \lambda_1. \quad (29)$$

The critical dynamics in Eqs. (28), (29) have the equilibria $(x, \lambda_1) = \left\{ (\pm 1, 0), (0, 0), \left(\pm \frac{1}{\sqrt{3}}, \mp \frac{2}{3\sqrt{3}} \right) \right\}$. Note that in the absence of noise, there is a path connecting the equilibria along the x axis. For nonzero noise, there is a heteroclinic connection in the x, λ_1 plane between the two states which represents the optimal path—the most likely trajectory for switching between the basins at $x = \pm 1$ and $x = 0$. For this system it is possible to solve for this path explicitly using a series of transformations. The optimal path for the x coordinate given as a solution to Eqs. (28), (29) is

$$x(t) = \pm \frac{1}{\sqrt{1 - A \exp(2t)}},$$

where A is an arbitrary coefficient to be determined by the initial condition. Due to symmetry, it suffices to study switching between either $x = \pm 1$ and $x = 0$; we choose to examine switching from -1 to 0 , i.e. the negative branch of $x(t)$. By inspection it is clear that $A < 0$, otherwise solutions would cease to exist in finite time. In calculating the action this coefficient is irrelevant. Choosing $A = -1$ (implying $x(0) = \frac{1}{2}$) without loss of generality results in the optimal path:

$$x(t) = -(1 + \exp(2t))^{-1/2}. \quad (30)$$

Integrating and solving for the arbitrary unknown functions, the Hamiltonian for the slow system is:

$$\mathcal{H} = (x - x^3)\lambda_1 + \lambda_1^2/2. \quad (31)$$

By inspection, we find that $\mathcal{H} = 0$ at both the origin and $(x, \lambda_1) = (\pm 1, 0)$. The equation for the curve connecting the two states is easily obtained from Eq. (31):

$$\lambda_1(x(t)) = 2(x(t))^3 - x(t).$$

One may calculate the action in the singular case by carrying out the integral $R(x) = \int_{-1}^0 \lambda_1(x) dx$. However, this would ignore the dependence of the action on the fast variables; to approximate this influence, we will resort to center manifold approximations.

IV. CENTER MANIFOLD REDUCTION

To analyze Eqs. (24)-(27), we will apply center manifold approximations to reduce the number of dimensions in the system. The system must first be rescaled to be placed in a form that is amenable for this process. To obtain the layer equations, we apply the scaling $t = \epsilon\tau$:

$$\lambda_1' = \epsilon(3x^2 - 1)\lambda_2 \quad (32)$$

$$\lambda_2' = \lambda_2 - \lambda_1 \quad (33)$$

$$y' = x - x^3 - y \quad (34)$$

$$x' = \epsilon(y + \lambda_1) \quad (35)$$

$$\epsilon' = 0. \quad (36)$$

One benefit of Eqs. (32)–(36) is that it is no longer singular as ϵ vanishes. A second benefit is that Eqs. (33)–(34) involve terms that are linear in the state variables (a space which now includes ϵ) and that all other equations are purely nonlinear. Therefore, the hypotheses of the center manifold theorem are satisfied and center manifold reductions may be applied to Eqs. (32)–(36) to reduce the dimensionality of the system [28] [33]. Since the vector field Eqs. (32)–(36) is smooth, we may assume:

$$y = h(x, \lambda_1, \epsilon) \quad (37)$$

$$\lambda_2 = k(x, \lambda_1, \epsilon) \quad (38)$$

where h and k are differentiable functions of the quantities specified. Applying the definitions in Eqs. (37), (38) to Eqs. (33)–(34) and substituting the vector fields in Eqs. (32), (35) when applying the chain rule, we obtain a system of two partial differential equations that may be solved for the unknown functions that will define the center manifold. These equations are known as the *center manifold conditions*. Beginning with the condition resulting from Eq. (34):

$$\left(\frac{\partial k}{\partial x} x' + \frac{\partial k}{\partial \lambda_1} \lambda_1' \right) = k(x, \lambda_1, \epsilon) - \lambda_1, \quad (39)$$

also for Eq. (33),

$$\left(\frac{\partial h}{\partial x} x' + \frac{\partial h}{\partial \lambda_1} \lambda_1' \right) = x - x^3 - h(x, \lambda_1, \epsilon). \quad (40)$$

In general, solving the partial differential Eqs. (40), (39) will be difficult. However, the center manifold reduction method next calls for making approximations for the functions h and k in terms of polynomials of increasingly higher order in their dependent variables. Each variable contributes to the order of a given term; to represent this, one may consider each variable scaled by a parameter α . The series is truncated at an arbitrarily specified order in α . Explicitly, this means:

$$\begin{aligned} h(x, \lambda_1, \epsilon) &= c_0 + \alpha(c_1 x + c_2 \epsilon + c_3 \lambda_1) + \alpha^2(c_4 x^2 + c_5 x \lambda_1 \\ &\quad + c_6 x \epsilon + c_7 \lambda_1^2 + c_8 \lambda_1 \epsilon + c_9 \epsilon^2) + \dots \\ k(x, \lambda_1, \epsilon) &= d_0 + \alpha(d_1 x + d_2 \epsilon + d_3 \lambda_1) + \alpha^2(d_4 x^2 + d_5 x \lambda_1 \\ &\quad + d_6 x \epsilon + d_7 \lambda_1^2 + d_8 \lambda_1 \epsilon + d_9 \epsilon^2) + \dots \end{aligned}$$

The center manifold expressions to fourth order in α and ordered by power in ϵ are:

$$h = x - x^3 - (x + \lambda_1 - 4x^3 - 3x^2\lambda_1)\epsilon + (2x + \lambda_1)\epsilon^2 + \mathcal{O}(|\alpha|^5) \quad (41)$$

$$k = \lambda_1 + (-\lambda_1 + 3x^2\lambda_1)\epsilon + (2\lambda_1 + 6x\lambda_1^2)\epsilon^2 - 5\lambda_1\epsilon^3 + \mathcal{O}(|\alpha|^5). \quad (42)$$

Note that setting $\epsilon = 0$ in the expressions for h and k in Eqs. (41), (42) recovers precisely the critical dynamics of Eqs. (28), (29). Since the expressions are given in powers of α , they do not represent an accounting of all terms that may be present for a given high order in ϵ . However, after taking the series in α to high enough order, low-order terms in ϵ stop appearing and the resulting series is treated as one in ϵ .

Numerical integration of the original system Eqs. (24)–(27) compared with its center manifold approximation (with y , λ_2 calculated using Eqs. (41), (42) respectively) gives remarkable agreement even at first order in ϵ . A plot of the integration is shown in Figure 1.

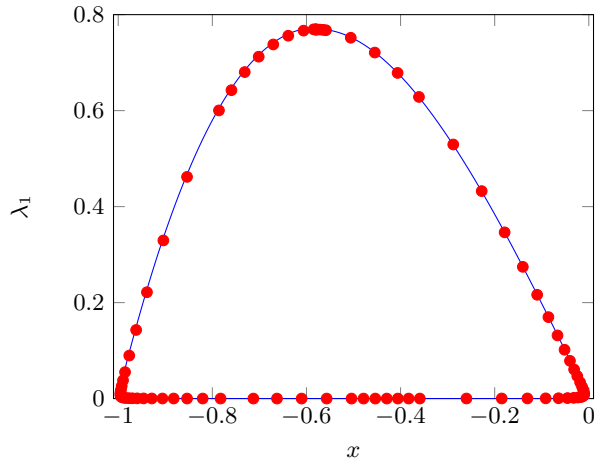


FIG. 1. Phase portraits of the full system in Eqs. (24)–(27) (blue line) compared with its center manifold approximation (red dots) for $\epsilon = 0.001$.

The action of noise along the optimal path in this system is:

$$\begin{aligned} \mathcal{R}[x, y, \eta, \lambda_1, \lambda_2] = & \frac{1}{2} \int_{-\infty}^{\infty} \eta^2(t) dt \\ & + \int_{-\infty}^{\infty} \lambda_1 (\dot{x} - f(x, y) - \eta(t)) dt \\ & + \int_{-\infty}^{\infty} \lambda_2 (\epsilon \dot{y} - g(x, y)) dt \end{aligned}$$

Having established approximations for these quantities previously as series expansions in ϵ , it is merely a

matter of careful substitution, differentiation and integration to obtain an approximation to the integral to arbitrary order in ϵ . First, substitutions may be made using the center manifold expressions $y = h(x, \lambda_1, \epsilon)$ and $\lambda_2 = k(x, \lambda_1, \epsilon)$ in Eqs. (39), (40). Second, apply the identity along the zero-Hamiltonian curve for $\lambda(t)$ as obtained in Eq. (31), along with $x(t)$ from Eq. (30). Differentiating and integrating as necessary results in the expression

$$\mathcal{R} = \frac{1}{2} - \frac{1}{4}\epsilon^2 + \mathcal{O}(\epsilon^3) \quad (43)$$

where the leading order term is the contribution from the singular case.

V. NUMERICAL RESULTS

To test the predictions resulting from this method, we compared the scaling predicted from the perturbation method with repeated stochastic simulation of the damped Duffing oscillator for various values of D and ϵ . The stochastic simulations were run using implicit numerical integration, the details of which are outlined in the Appendix.

It is convenient to make comparisons between numerics and analytical approximations by analyzing the logarithm of the escape time across multiple orders of magnitude. A plot of the stochastic simulations compared against the escape time as predicted using the perturbation method is shown in Figure 2; the two methods agree very well. Table I provides a side-by-side comparison of the scaling coefficient between the MFPT and ϵ as calculated by the perturbation method and from linear regression of stochastically simulated switching. The error bounds represent the standard deviation on the slope of the regression line.

ϵ	Scaling coefficient $C_S \times 10^2$	
	perturbation method	stochastic simulation
0.001	10.86	10.91 \pm 1.213
0.003	10.86	10.84 \pm 1.370
0.01	10.86	10.79 \pm 1.034
0.1	10.80	10.80 \pm 1.246
0.2	10.64	10.60 \pm 1.189
0.5	9.500	9.295 \pm 1.107
1.0	5.428	6.469 \pm 0.9437

TABLE I. Comparison of scaling coefficients for MFPT between the perturbation method and stochastic simulation. The scaling law is assumed to be $\log_{10}(T_S) = C_S(1/D) + b$, where b is a constant determined by simulation. The data above quantify the predictions and observations in Figure 2.

As shown in Table I, the agreement between stochastic simulation and the perturbation method is quite good and well within the standard deviation for the slope of the

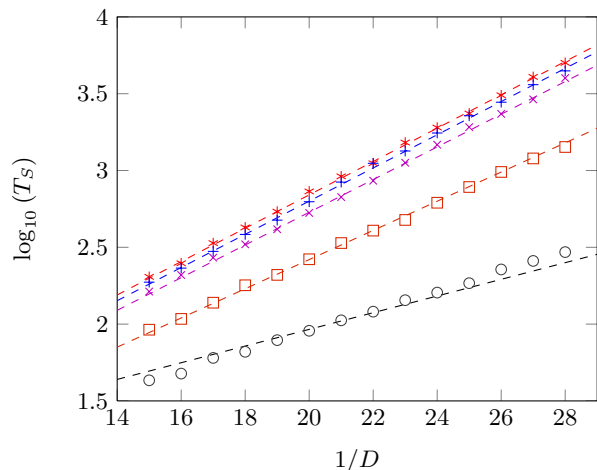


FIG. 2. Mean first passage times from a potential well varying with ϵ and D . Data points were computed as an ensemble average of 1000 trials. \circ represents $\epsilon = 1.0$, \square $\epsilon = 0.5$, \times $\epsilon = 0.2$, $+$ $\epsilon = 0.1$ and $*$ $\epsilon = 0.01$. Color-corresponding lines show the perturbation-predicted escape times. Lines have been shifted to allow comparison with the slopes of simulation data.

regression line. However, as the timescales are brought into alignment with one another, the center manifold approximation applied to the slow system becomes a poor approximation for the system dynamics. This can be confirmed visually by observing that the agreement for $\epsilon = 1.0$ in Figure 2 is not strong.

VI. DISCUSSION

Figure 2 shows that the method fails to predict the mean first passage time if ϵ is too large. Both ϵ and D are assumed to be small for the perturbation series and simplifications made. The magnitude of the noise intensity D may be compared with the height of the barrier through which the particle must traverse to switch states. The approximations made do not apply to events where noise is so significant as to typically cause a transition or where there is little separation between the time scales. However, the process may be applied to even higher-dimensional systems where the time scale separation translates into a spectral gap in relaxation times.

In the regime where D is large compared to the height of the barrier, the mean first passage time will rapidly decrease. This behavior cannot be captured by the WKB approximation ansatz; the Eikonal approximation can only capture a linear relationship between $\log T_S$ and $1/D$. A method could be developed to obtain statistics about slow-fast stochastic systems when D is significant compared to the effective barrier height, and this will be left to future work in which noise is finite and large.

These restrictions aside, the method is resilient to choices of vector field. Despite the Duffing oscilla-

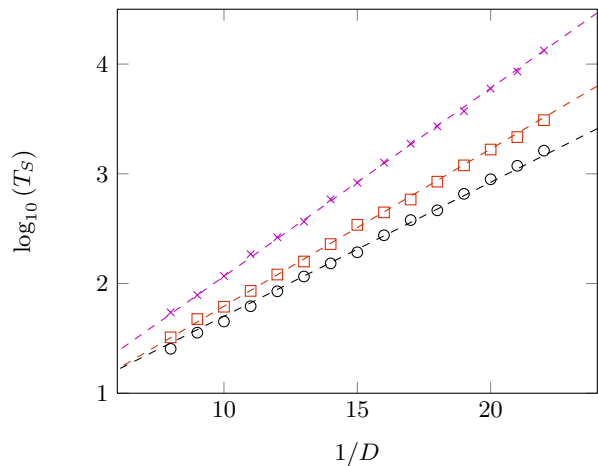


FIG. 3. Mean first passage times from a potential well varying with ϵ and D . Data points were computed as an ensemble average of 1000 trials. \circ represents $\epsilon = 0.5$, \square $\epsilon = 0.4$, \times $\epsilon = 0.2$.

tor's symmetry, the method has been applied to another double-welled system with broken symmetry and has resulted in similarly good agreement. Our test system was an unsymmetric Duffing-like oscillator with differential equations:

$$\dot{x} = y + \eta(t) \quad (44)$$

$$\epsilon \dot{y} = x(1+x)(2-x) - y. \quad (45)$$

The system in Eqs. (44), (45) has two stable equilibrium points at $x = -1$ and $x = 2$ separated by a saddle at $x = 0$. The method outlined in this paper gives the approximate expression for the action of:

$$\mathcal{R} = \frac{5}{6} - \frac{13}{12}\epsilon^2 + \mathcal{O}(\epsilon^3).$$

A comparison of numerically- and formally-generated results for the mean first passage time in this system is provided in Figure 3. Both examples we have carried out do not have any $\mathcal{O}(\epsilon)$ terms appearing in the approximation to the action; this may be understood via an analogy with function optimization. The local behavior of a function at a minimum with respect to a parameter has no linear dependence on said parameter by definition.

A contemporary and popular approach to obtain similar results for the occurrence of rare events uses what are known as sample-based techniques. Throughout our approach, we have completely avoided the use of such methods. These approaches generally have required the calculation of convolution integrals that depend on the realization of noise for all past and future times; while analytically tractable, this comes with some assumptions. Some of the integrals that result from sample-base approaches must remain bounded, putting further restrictions on the noise distribution. Such restrictions

can be challenging to rigorously justify and are at times opaque. Our approach does not require such justifications and reaches complementary conclusions while remaining transparent throughout the process, making it a useful and very straightforward alternative to sample-based techniques.

Finally, the use of center manifold reductions requires considerable algebraic manipulation that may not be tenable in all circumstances, e.g. in high dimensional systems or those with many parameters. Such systems often have lower-dimensional analogs which may be amenable to this analysis and thus are within reach of this method. However, there are other approaches. For instance, computational methods exist to minimize the action in a variety of gradient and non-gradient systems [34]. These numerical algorithms provide a new approach to verify the scaling relationships generated by our method in theory and experiment.

VII. CONCLUSION

In this work, a method was developed to leverage the disparate timescales in slow-fast stochastic systems to aid analysis and predict switching times between attractors. The process avoided the projection of noise vectors onto the slow manifold in favor of analyzing the noisy system via a variational approach to find the optimal path. The damped Duffing oscillator was used as an example of a prototypical system with two potential wells where switching can occur as a result of large fluctuations. Using this theory, we transformed the original 2-dimensional stochastic system into a 4-dimensional deterministic system and proceeded to analyze the optimal path representing the most likely noise to induce a transition. The action along this path was crucial to determining the switching time between the two metastable states present.

For future work, we intend to apply this theory to prescient examples of slow-fast stochastic systems, including epidemic models with non-Gaussian noise. We also will apply this method to systems which exhibit delayed feedback.

VIII. ACKNOWLEDGEMENTS

The authors gratefully thank Luis Mier-y-Teran Romero for helpful discussions and his prescient insight. This research was performed while CRH held a National Research Council Research Associateship Award at the U.S. Naval Research Laboratory. This research is funded by the Office of Naval Research contract F1ATA01098G001 and by Naval Research Base Program Contract N0001412WX30002.

Appendix A: Stochastic simulations

Ordinary differential equations with multiple timescales present unique challenges when numerically integrating to obtain a time series, including the possibility of the system's being "stiff." Stiffness is a qualitative property of a dynamical system that stymies standard (i.e. explicit) numerical integration methods. This effect may be illustrated with a simple example; consider the system of differential equations:

$$\dot{\mathbf{x}} = \mathbf{F}(\mathbf{x}, \mathbf{y}) + \alpha \Phi \quad (\text{A1})$$

$$\epsilon \dot{\mathbf{y}} = \mathbf{G}(\mathbf{x}, \mathbf{y}) \quad (\text{A2})$$

where $\mathbf{x} \in \mathbb{R}^m$, $\mathbf{y} \in \mathbb{R}^n$, \mathbf{F} and \mathbf{G} are differentiable functions, Φ is a white noise term with amplitude controlled by α and ϵ is a parameter that tunes the separation of the timescales between the variables \mathbf{x} and \mathbf{y} . For the purpose of illustration, we first set $\alpha = 0$. To obtain a time series of Eqs. (A1), (A2) there are many numerical recipes that may be applied, the simplest of which is Euler's Method. Let \mathcal{D} represent taking the Jacobian of the vector field, and let $\mathcal{D}\mathbf{F}$, $\mathcal{D}\mathbf{G}$ be nonsingular. Euler's Method calls for generating successive iterations of the underlying function by discretizing time with a uniform step size ν and iterating the resulting map:

$$\mathbf{x}_{k+1} = \mathbf{x}_k + \nu \mathbf{F}(\mathbf{x}_k, \mathbf{y}_k) \quad (\text{A3})$$

$$\mathbf{y}_{k+1} = \mathbf{y}_k + \frac{\nu}{\epsilon} \mathbf{G}(\mathbf{x}_k, \mathbf{y}_k) \quad (\text{A4})$$

In general, the eigenvalues of both $\mathcal{D}\mathbf{F}$, $\mathcal{D}\mathbf{G}$ are $\mathcal{O}(1)$. Of particular concern is the factor of $\frac{\nu}{\epsilon}$, which is generally very large. The eigenvalues of Eq. (A4) will in general be much larger than those of Eq. (A3), which leads to stiffness. This inverse relationship between ν and ϵ creates a numerical quandary since the necessary step size to ensure stability is $\mathcal{O}(\epsilon)$, which is arbitrarily small. For accuracy, step sizes must be chosen much smaller than this necessary step size, further aggravating the numerical challenges.

To circumvent this complication, implicit methods are often used to solve for the state of the system after a time step. We now re-introduce noise by setting $\alpha = 1$ and draw the noise \mathbf{W}_k at step k from a Gaussian distribution with mean 0 and standard deviation 1. Using a first-order Milstein method, the implicit recipe used in our stochastic simulations is:

$$\mathbf{x}_{k+1} = (\mathbf{x}_k, \mathbf{y}_k) + \nu \mathbf{F}(\mathbf{x}_{k+1}, \mathbf{y}_{k+1}) + \sqrt{\nu} \mathbf{W}_k \quad (\text{A5})$$

$$\mathbf{y}_{k+1} = (\mathbf{x}_k, \mathbf{y}_k) + \frac{\nu}{\epsilon} \mathbf{G}(\mathbf{x}_{k+1}, \mathbf{y}_{k+1}) \quad (\text{A6})$$

Solving for $(\mathbf{x}_{k+1}, \mathbf{y}_{k+1})$ in Eqs. (A5), (A6) is an exercise in nonlinear, multidimensional root-finding. Since we expect the system's value at two adjacent timesteps

to be close, we may take ν arbitrarily small such that a Newton-Raphson iterative scheme will converge to the value of \mathbf{x}_{k+1} . While the iterative scheme converges quickly, this still involves significant computational overhead since it in general requires the inversion of a large matrix.

To compute the mean first passage time for the stochastic systems compared in Fig. 2, the implicit recipe provided in Eqs. (A5), (A6) was used to integrate the

system until noise caused it to escape from the potential well. The first passage time was recorded, and the system was reset. This ensemble was run for 1,000 simulations for each value of ϵ and D and the mean of all first passage times for the given parameter values was computed. The total computation time was considerable even on a desktop PC with 8 processors using MATLAB's parallel computing toolbox. The processing time to generate Figure 2 was over two weeks using all eight cores clocked at 2.8 GHz.

-
- [1] M. Desroches, J. Guckenheimer, B. Krauskopf, C. Kuehn, H. M. Osinge, and M. Wechselberger, *SIAM Review* **54**, 211 (2012).
- [2] L. Gammaitoni, P. Hänggi, P. Jung, and F. Marchesoni, *Rev. Mod. Phys.* **70**, 223 (1998).
- [3] H. B. Chan, M. I. Dykman, and C. Stambaugh, *Physical Review E* **78**, Art. no. 051109 (2008).
- [4] M. I. Dykman, *Phys. Rev. A* **42**, 2020 (1990).
- [5] M. I. Dykman, P. V. E. McClintock, V. N. Smelyanski, N. D. Stein, and N. G. Stocks, *Phys. Rev. Lett.* **68**, 2718 (1992).
- [6] M. Millonas, ed., *Fluctuations and Order: The New Synthesis* (Springer-Verlag, 1996).
- [7] D. G. Luchinsky, P. V. E. McClintock, and M. I. Dykman, *Rep. Prog. Phys.* **61**, 889 (1998).
- [8] R. P. Feynman and A. R. Hibbs, *Quantum Mechanics and Path Integrals* (McGraw-Hill, Inc., 1965).
- [9] M. I. Freidlin and A. D. Wentzell, *Random Perturbations of Dynamical Systems* (Springer-Verlag, 1984).
- [10] W. E, *Principles of Multiscale Modeling* (Cambridge University Press, 2011).
- [11] A. Wentzell, *Theor. Probab. Appl.* **21**, 227 (1976).
- [12] G. Hu, *Phys. Rev. A* **36**, 5782 (1987).
- [13] M. I. Dykman, E. Mori, J. Ross, and P. M. Hunt, *J. Chem. Phys.* **100**, 5735 (1994).
- [14] R. Graham and T. Tél, *Phys. Rev. Lett.* **52**, 9 (1984).
- [15] R. S. Maier and D. L. Stein, *Phys. Rev. E* **48**, 931 (1993).
- [16] A. Hamm, T. Tél, and R. Graham, *Physics Letters A* **185**, 313 (1994).
- [17] N. Berglund and B. Gentz, *Noise-Induced Phenomena in Slow-Fast Dynamical Systems: A Sample-Paths Approach* (Springer-Verlag, 2006).
- [18] P. Boxler, *Probab. Theory Rel.* **83**, 509 (1989).
- [19] E. Knobloch and K. A. Wiesenfeld, *J. Stat. Phys.* **33**, 611 (1983).
- [20] N. S. Namachchivaya, *Appl. Math. Comput.* **38**, 101 (1990).
- [21] N. S. Namachchivaya and Y. K. Lin, *Int. J. Nonlinear Mech.* **26**, 931 (1991).
- [22] L. Arnold and P. Imkeller, *Probab. Theory Rel.* **110**, 559 (1998).
- [23] L. Arnold, *Random Dynamical Systems* (Springer-Verlag, 1998).
- [24] Y. Kabanov and S. Pergamenschikov, *Two-Scale Stochastic Systems: Asymptotic Analysis and Control* (Springer-Verlag, 2003).
- [25] A. J. Roberts, *Physica A* **387**, 12 (2008).
- [26] E. F. Forgoston and I. B. Schwartz, *SIAM J. App. Dyn. Syst.* **8**, 1190 (2009).
- [27] J. Guckenheimer, K. Hoffman, and W. Weckesser, "Bifurcations of relaxation oscillations near folded saddles," (2004).
- [28] J. Carr, *Applications of Centre Manifold Theory* (Springer-Verlag, 1981).
- [29] C. W. Gardiner, *Handbook of Stochastic Methods for Physics, Chemistry and the Natural Sciences* (Springer-Verlag, 2004).
- [30] G. Weiss, ed., "Contemporary problems in statistical physics," (Society for Industrial and Applied Mathematics, 1994) Chap. 2.
- [31] M. I. Dykman, *Physical Review E* **81**, Art. no. 051124 (2010).
- [32] T. J. Kaper, *Proceedings of Symposia in Applied Mathematics* **56** (1999).
- [33] J. Guckenheimer and P. Holmes, *Nonlinear Oscillations, Dynamical Systems, and Bifurcations of Vector Fields* (Springer-Verlag, 1997).
- [34] W. E, W. Ren, and E. Vanden-Eijnden, *Communications on Pure and Applied Mathematics* **57**, 637 (2004).